

# The True Amphipathic Nature of Graphene Flakes: A Versatile 2D Stabilizer

Anna W. Kuziel, Karolina Z. Milowska,\* Pak-Lee Chau, Slawomir Boncel, Krzysztof K. Koziol,\* Noorhana Yahya, and Mike C. Payne

The fundamental colloidal properties of pristine graphene flakes remain incompletely understood, with conflicting reports about their chemical character, hindering potential applications that could exploit the extraordinary electronic, thermal, and mechanical properties of graphene. Here, the true amphipathic nature of pristine graphene flakes is demonstrated through wet-chemistry testing, optical microscopy, electron microscopy, and density functional theory, molecular dynamics, and Monte Carlo calculations, and it is shown how this fact paves the way for the formation of ultrastable water/oil emulsions. In contrast to commonly used graphene oxide flakes, pristine graphene flakes possess well-defined hydrophobic and hydrophilic regions: the basal plane and edges, respectively, the interplay of which allows small flakes to be utilized as stabilizers with an amphipathic strength that depends on the edge-to-surface ratio. The interactions between flakes can be also controlled by varying the oil-to-water ratio. In addition, it is predicted that graphene flakes can be efficiently used as a new-generation stabilizer that is active under high pressure, high temperature, and in saline solutions, greatly enhancing the efficiency and functionality of applications based on this material.

Since the experimental proof of its existence,<sup>[1]</sup> graphene, a 2D carbon allotrope, has attracted a vast amount of research activity due to its unique electronic, mechanical, and thermal properties.<sup>[2]</sup> This extraordinary material holds great promise for applications ranging from optoelectronic, through environmental to biomedical technologies. To efficiently manufacture graphene-based devices, composites, coatings, or membranes, it is essential to understand graphene's properties and, for


many applications, its interactions with adsorbates when it is placed in a liquid environment. To date, nearly all studies focused on graphene oxide (GO) flakes or its derivatives obtained by subsequent reduction or further functionalization<sup>[3,4]</sup> rather than on pure graphene flakes. This is primarily because pristine graphene is considered as difficult to disperse and individualize in solvents, melts, and matrices. However, graphene oxide flakes, which have no clearly defined structure, are not only difficult to process,<sup>[5]</sup> toxic,<sup>[6]</sup> but also do not retain the fundamental properties of graphene. A recent study<sup>[4]</sup> has also shown that graphene oxide cannot be considered as a true 2D stabilizer. The presence of additional stabilizing highly oxidized carbon material, the so-called oxidative debris, adsorbed on the surface of the graphene oxide flake, is a prerequisite for graphene oxide flakes to stabilize an

emulsion.<sup>[7]</sup> Therefore, broader utilization of pristine graphene would have major advantages in terms of applications.

Despite significant progress in the field in recent years, there is no consensus whether graphene flakes are typical hydrophobes<sup>[8]</sup> or could, under certain conditions, become wetttable.<sup>[9,10]</sup> There is also much debate about which parameter plays a dominant role in tuning the hydrophobicity: lateral size,<sup>[11]</sup> number of layers<sup>[9]</sup> or a combination of specific surface area and thickness

A. W. Kuziel, Prof. K. K. Koziol  
Enhanced Composites and Structures Center  
School of Aerospace  
Transport and Manufacturing  
Cranfield University  
Bedfordshire MK43 0AL, United Kingdom  
E-mail: k.koziol@cranfield.ac.uk

A. W. Kuziel, Prof. S. Boncel  
Faculty of Chemistry  
Silesian University of Technology  
Krzywoustego 4, Gliwice 44-100, Poland

 The ORCID identification number(s) for the author(s) of this article can be found under <https://doi.org/10.1002/adma.202000608>.

© 2020 The Authors. Published by WILEY-VCH Verlag GmbH & Co. KGaA, Weinheim. This is an open access article under the terms of the Creative Commons Attribution License, which permits use, distribution and reproduction in any medium, provided the original work is properly cited.

DOI: 10.1002/adma.202000608

Dr. K. Z. Milowska, Prof. M. C. Payne  
TCM Group  
Cavendish Laboratory  
University of Cambridge  
19 JJ Thomson Avenue, Cambridge CB3 0HE, United Kingdom  
E-mail: kzm21@cam.ac.uk

Dr. P.-L. Chau  
Bioinformatique Structurale  
Institut Pasteur  
CNRS URA 3528  
CB31 CNRS USR 3756  
Paris 75724, France

Prof. N. Yahya  
Department of Fundamental and Applied Sciences  
Universiti Teknologi PETRONAS  
32610 Seri Iskandar, Perak Darul Ridzuan, Malaysia

of flakes.<sup>[12,13]</sup> Moreover, some studies even suggest that pristine graphene flakes are a new type of stabilizer which can stabilize the oil/water emulsions<sup>[13,14]</sup> without any additional agents enabling their assembly at the oil/water interface.<sup>[12]</sup>

Therefore, we have reinvestigated this question with precise experiments and rigorous theoretical studies. Here, we demonstrate the amphiphatic nature of pristine graphene flakes and how to tune it by varying the flake size. In doing this, we explain all the reported inconsistencies in the literature. We discuss the underlying mechanism responsible for the stability of water/oil emulsions stabilized by pristine graphene flakes and its dependence on the water-to-oil ratio. Moreover, we show the versatile and robust character of pristine graphene flakes which enables them to function under extreme conditions. This makes graphene flakes promising candidates for dispersing agents in the preparation of polymer or ceramic composites, heat transfer fluids, paints, conductive catalyst supports, filters, drug nanocarriers in cancer therapy, and new generation of stabilizers for geological applications.

For the macroscopic studies of the oil–water interphase behavior of graphene flakes, we have chosen two types of graphene flakes which according to the ISO/TS 80004-13:2017 norm may be understood as mono-, bi-, tri-, and few-layer graphene. G1 graphene flakes have thicknesses in the range of 0.3–1.7 nm, with approximately 70% being single layers, and surface areas of approximately  $320 \pm 20 \text{ m}^2 \text{ g}^{-1}$  (measured using Brunauer–Emmett–Teller theory of bulk samples), G3 flakes have a smaller surface areas of about  $130 \pm 5 \text{ m}^2 \text{ g}^{-1}$ , while their thickness is slightly larger than 1–5 nm. Both types of flakes (Figure 1A) are practically non-wettable by deionized water and are instantly dispersible in *n*-decane, a model of an oil phase. Optical photographs and microscopy images presented in Figure 1A and Figure S1, Supporting Information, show that both types of graphene flakes agglomerate in an aqueous solution. Optical microscopy analysis revealed that the dispersibility of G3 flakes (thicker and of smaller surface area) in *n*-decane is significantly higher than G1 flakes (cf. left panels in Figure S1A,B, Supporting Information). In

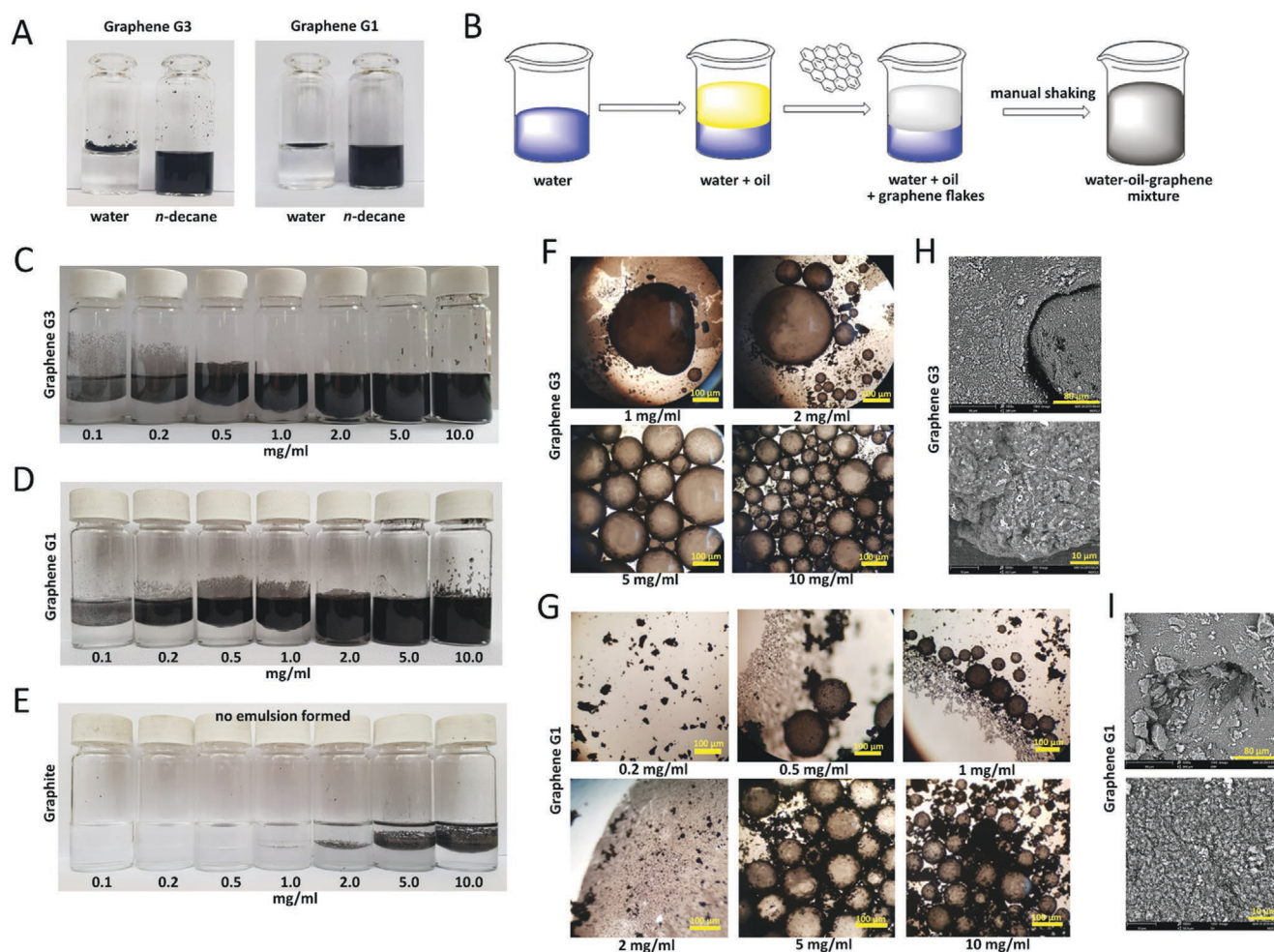


**Figure 1.** Formation of water/oil emulsions stabilized by graphene flakes A) Dispersibility of graphene in water and *n*-decane immediately after adding graphene flakes to liquids. B) Schematic illustration of preparation of water/oil emulsions. C,D) Optical photographs of Pickering emulsions stabilized by various concentrations of graphene flakes G3 and G1 in water/*n*-decane mixtures, and E) the corresponding samples containing graphite flakes. In contrast to graphene, graphite flakes show non-dispersible and non-emulsifying character in water/oil mixtures. F,G) Optical microscopy images of graphene flakes G3 and G1 stabilized emulsion droplets. H,I) SEM images of lyophilized graphene G3 and G1 nanostructures, respectively. The spheroidal shapes of fragments of nanostructures are observed only in the case of G3.

contrast to G3, G1 flakes form agglomerates which were seen to be larger and thus were slightly less easily dispersed. This demonstrates that the performance of graphene flakes depends on their surface areas.

When placed into the equivolometric, biphasic *n*-decane/water mixture, both types of graphene flakes, diffuse only in the nonpolar phase, *n*-decane. However, manual shaking of experimental vials was found to produce an emulsion, as schematically presented in Figure 1B. Since the sine qua non condition for a substance to behave as an emulsifying agent is to exhibit amphiphatic character,<sup>[15]</sup> this simple experiment demonstrates that graphene flakes must be amphiphiles. Presumably, graphene flakes enable emulsification by formation of the outer layer of quasi-spherical domains (Figure 1F,G). Additionally, graphene flakes form thin films on the untreated hydrophilic glass vial above the level of the mixture (Figure 1C,D). This was also observed by Woltornist et al.<sup>[14]</sup>

To determine which liquid forms the droplet phase, optical microscopy images have been acquired on mixtures containing trace amounts of reddish hexahydrate of cobalt(II) nitrate(V) dissolved in the aqueous phase (Figure S2A, Supporting Information). The analysis of images which proved that the reddish aqueous phase constitutes the core of dispersed domain, that is, it is present inside the quasi-globules. Moreover, emulsion droplets added to *n*-decane remained intact, but they completely and immediately collapsed after being added to water (Figure S2B,C, Supporting Information). This confirms previous predictions<sup>[13,14]</sup> that graphene flakes stabilize water-in-oil emulsions and not oil-in-water emulsions which are stabilized by GO flakes.<sup>[5,16]</sup>

This simple experiment also shows that the individual droplets can be separated from the emulsions and placed in water or in *n*-decane, thus making possible to produce thin continuous films of graphene<sup>[14]</sup> for green chemistry applications.

To study the effect of the size and concentration of graphene flakes on the nature of the emulsions, we have prepared three sets of samples containing different concentrations of G3 and G1 graphene flakes and also commercial graphite flakes (+100 mesh). Unlike graphene flakes, graphite flakes cannot stabilize water/oil emulsions. They do not form the shells of droplets presumably because graphite flakes are too thick and too large. G3 graphene flakes, which are characterized by smaller surface areas than G1, yielded thermodynamically stable emulsions even when their concentration in the water/oil mixture was low. In contrast, G1 graphene flakes produced unstable emulsions at concentrations below 1 mg mL<sup>-1</sup>. As clearly seen in Figure 1G, at a G1 concentration of 0.2 mg mL<sup>-1</sup>, shells composed of G1 flakes collapsed leaving agglomerated flakes indicating that G1 flakes are more difficult to disperse in solvents. Comparison of optical microscopy images of emulsions prepared using these flakes (cf. Figure 1F,G) shows agglomerated flakes in G1 samples even at high concentrations of graphene flakes. This suggests that the bigger G1 shells broke down leaving only smaller shells intact and/or only a fraction of the flakes remained unemulsified.<sup>[13]</sup> This, in turn, suggests that the surface area of the flake is the most important parameter that determines its tendency to agglomerate and hence the interaction with water/oil mixtures.

Closer inspection of emulsions stabilized by G3 graphene flakes revealed that the size of graphene agglomerates protecting the droplets increases with decreasing concentration

of flakes (Figure 1F). At low concentrations of flakes, when large droplets are formed, graphene shells bigger than 250 μm collapse leaving thin graphene films. Such emulsions can be described as loose emulsions. At higher concentrations of flakes, the droplets become tighter and more uniform, but some discontinuities in the droplet coverage could still be observed (Figure 1F, bottom left panel). Apart from spherical structures, we also observed unbounded graphene flakes between droplets (Figure 1F, bottom right panel). These flakes might additionally have a role in stabilizing a 3D network of droplets.

To further investigate the structure of graphene flake assemblies, we have subjected emulsions stabilized by both type of flakes to lyophilisation and SEM analysis. Results for G3 and G1 flakes are presented in Figures 1H and 1I, respectively. Unfortunately, this procedure does not allow us to preserve the structure of a full shell. Therefore, SEM images show only fragments of flake-based droplet shell skeletons. Regardless of the graphene flake concentration, fragments of shells composed of G3 graphene flakes (in contrast to these formed of G1) have spheroidal shape and individual flakes are still densely clustered. This can be explained by the smaller surface area of G3 graphene flakes and hence stronger interactions between G3 flakes.

Boehm analysis<sup>[17]</sup> of the G3 flakes before and after mixing (Supporting Information) shows that graphene flakes remained chemically unaltered. This suggests that the mechanism of interactions and thus assembly into the observed spherical shells must be completely different from the GO flakes which form nonspherical shells<sup>[4,5]</sup> and connect through hydroxyl and/or carboxyl groups.<sup>[7,18]</sup>

To understand the mechanism responsible for the amphiphatic nature of graphene flakes and their assembly in the oil/water mixture, we performed density functional theory (DFT), molecular dynamics (MD), and Monte Carlo (MC) calculations on various oil/water/graphene flake systems.

We firstly used DFT to rigorously determine the interaction energy ( $E_{\text{int}}$ ) between graphene flakes, water and decane. Since the properties of nanocarbons vary significantly with their size, shape and edge topology<sup>[19]</sup> and graphene flakes possess two electrochemically distinctive regions: the basal plane surface, composed of conjugated sp<sup>2</sup> carbon atoms, and the edges, containing carbon atoms with dangling bonds,<sup>[20]</sup> we have considered both solvent molecules positioned above the surface and next to the edge of ten different graphene flakes. DFT calculations of eight graphene flakes ( $\Gamma_1$ – $\Gamma_8$ ) with lateral dimensions in the range of 1–2 nm but different shapes and edges (Figure 2A) show that the interactions between oil and flake surface are stronger ( $E_{\text{int}}$  is more negative) than between the oil and flake edges, regardless of the shape of flake or type of edge. The differences in interaction between different type of edges (see left panel in Figure 2A) and decane molecule are small (less than 0.072 eV) compared to the differences between surface and edge positions (1.306 eV for  $\Gamma_1$ ). In contrast, water molecules preferentially interact with flake edges rather than its surface. The oxygen atom of the water molecule is preferentially directed toward the edge of the flake, whereas in surface configurations, the hydrogen atoms are positioned closer to the flake carbon atoms. In the latter position at the minimum energy configuration, the water molecule is further from the graphene flake than in the edge configuration

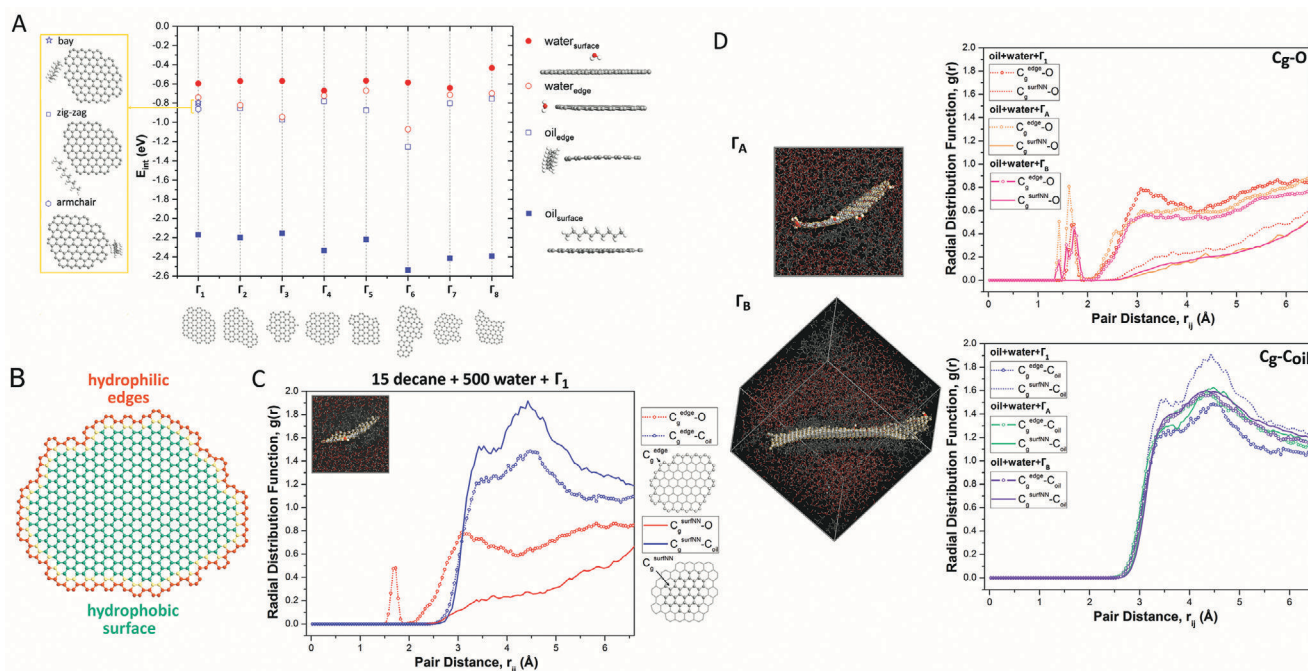


**Figure 2.** Interactions of graphene flakes with oil and water. A) Interaction energies for eight different small graphene flakes calculated in the framework of DFT. Oil prefers the top orientation (above the flake) whereas water prefers the edge orientation (next to the flake). Left: Atomistic views of three different fully optimized edge orientations of decane molecule next to  $\Gamma_1$  flake. Right: Visualisations of four types of systems used to study interactions between graphene flakes with oil and water molecules. The C atoms are depicted in dark grey while O and H are shown in red and white, respectively. B) Schematic diagram explaining the amphiphatic nature of graphene flake. Hydrophilic edges of graphene flake are marked in orange color, while hydrophobic basal plane in turquoise color. The properties of yellow atoms do not fully resemble the properties of surface atoms (Figure S4, Supporting Information). C) Left: RDF of edge carbon–water oxygen, surface carbon–water oxygen, edge carbon–oil carbon, and surface carbon–oil carbon atoms. The inset shows the snapshot of the final configuration. Water and oil molecules are represented as a stick model whereas graphene flake is displayed as a ball-and-stick model. Right: schematic diagrams showing edge ( $C_g^{\text{edge}}$ ) and chosen surface ( $C_g^{\text{surfNN}}$ ) atoms in  $\Gamma_1$  graphene flake. All carbon atoms constituting graphene flake edges are taken to the  $C_{\text{edge}}$  subset, whereas the  $C_{\text{surfNN}}$  subset is defined as a subset containing graphene flake carbon atoms except for all edge atoms and their nearest neighbours. D) RDFs for different size of graphene flakes. The snapshots of final configurations of simulation boxes containing bigger flakes,  $\Gamma_A$  and  $\Gamma_B$ , are displayed on the left. All RDFs are calculated from MD simulations at 300 K and 1 bar.

(Table S1, Supporting Information). The structural analysis also shows that the H–O bond length of water increases by 0.01 Å when the water molecule is in the edge orientation and the H–O–H angles of water in the edge configuration are bigger than in the surface configuration. Moreover, the changes in the electron density of the graphene flake are only visible in the edge configuration (Figure S4, Supporting Information). The presence of additional hydroxyl and epoxy groups attached to the flake edges reduces the energy differences between different orientations of the oil and water molecules (Figure S5, Supporting Information). These results clearly indicate that the surface of the basal plane of graphene flakes is hydrophobic while edges are hydrophilic, as presented in Figure 2B.

To gain further insight into the amphiphatic character of graphene flakes, we have performed MD calculations of all small graphene flakes ( $\Gamma_1$ – $\Gamma_8$ ) in oil/water mixtures as described in Supporting Information. Figure 2C shows the radial distribution function (RDF) between edge carbon–water oxygen, surface carbon–water oxygen, edge carbon–oil carbon, and surface carbon–oil carbon atoms for a system containing a  $\Gamma_1$  flake. The first peak in the  $C_g^{\text{edge}}\text{--O}$  RDF appears at 1.70 Å indicating on an edge functionalization by oxygen-bearing groups. It is a consequence of the interatomic potential used and such a process is not observed in experiments. However, note that provided

G3 flakes contain a small number of oxygen atoms (see Boehm analysis in the Supporting Information). The second and the third peaks in the  $C_g^{\text{edge}}\text{--O}$  RDF have values 0.18 at 2.45 Å and 0.88 at 3.15 Å. These are associated with the water oxygen atoms close to the edge carbon atoms. The first peak of the  $C_g^{\text{surfNN}}\text{--O}$  RDF does not appear until 3.58 Å and it has value of only 0.23. On the other hand, the first peak in the  $C_g^{\text{edge}}\text{--C}_{\text{oil}}$  RDF has value of 1.43 at 3.59 Å, whereas the first peak in the  $C_g^{\text{surfNN}}\text{--C}_{\text{oil}}$  RDF is 1.68 at 3.47 Å. In agreement with DFT results, MD simulation shows that water molecules are located in the direct vicinity of graphene flake edges whereas oil molecules are positioned above and below the basal plane. Clearly, the surface of the flake attracts more oil molecules than the edges and the smallest distance between oil carbon atoms and flake surface carbon atoms is smaller than between oil carbon and flake edge carbon atoms. It is also worth noticing that the graphene flake is no longer flat.

Since the hydrophilic nature of the flake is associated only with graphene flake edges and the hydrophobic character only with the surface of flake, one may expect a size-dependent amphiphilicity of graphene flakes. While small GO flakes (<1 μm) are not capable of stabilizing emulsion droplets due to reduction of hydrophobic islands on their basal plane surfaces and, in consequence, their amphiphilicity,<sup>[16,22,23]</sup> only small pristine graphene flakes, due to their high edge-to-surface ratio,

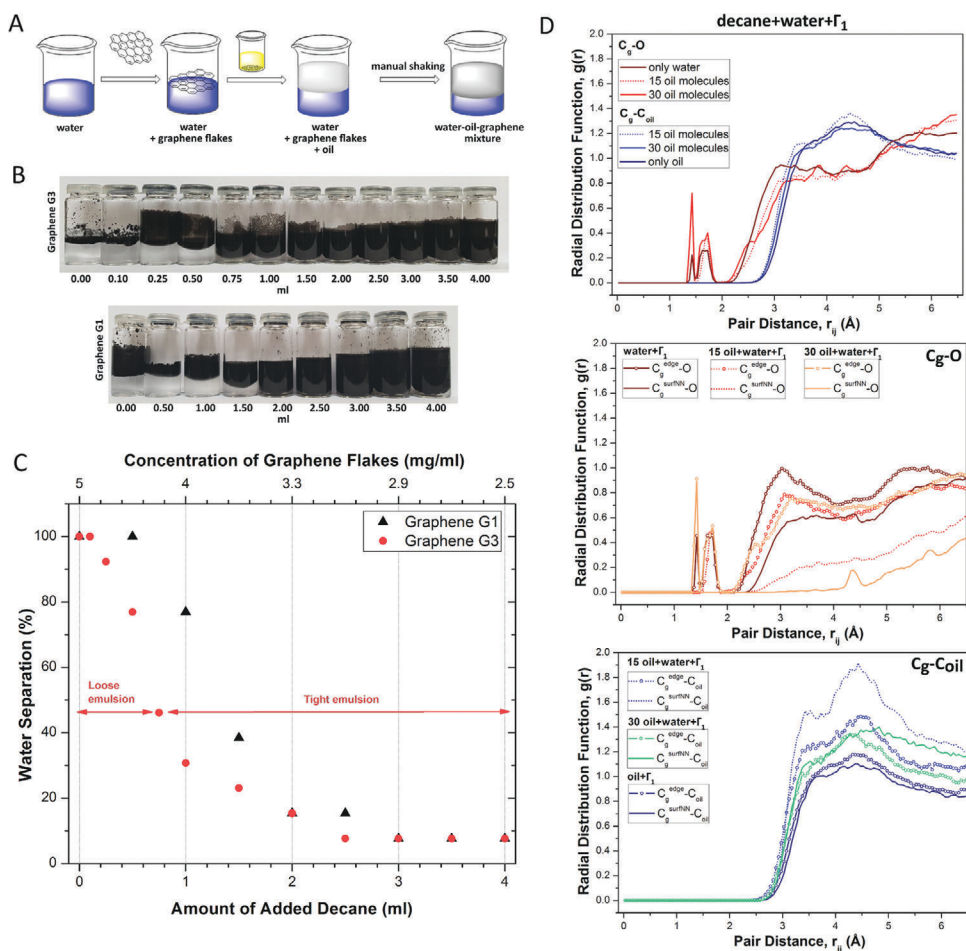


**Figure 3.** Effect of oil–water ratio on the stability of water/oil emulsions. A) Experimental protocol for studying the stability of water/oil emulsions stabilized by graphene flakes. B) Optical photographs of Pickering emulsions stabilized by graphene flakes G3 and G1 with varying amounts of added *n*-decane. C) The percentage separation of the aqueous phase as a function of added *n*-decane. The top axis shows the corresponding concentrations of graphene flakes. D) RDFs for  $\Gamma_1$  flakes in different oil–water ratios at 300 K and 1 bar.

should have sufficient amphipathic strength to exhibit good emulsifying capabilities. To test this hypothesis, we have performed DFT and subsequent MD simulations of two bigger graphene flakes,  $\Gamma_A$  and  $\Gamma_B$  of approximately 4–5 nm and 5–6 nm in diameter (Figure S7, Supporting Information). While the DFT calculations do not present a clear trend in the amphipathic strength as a function of flake size (Figure S7, Supporting Information), the MD simulations show that interactions between the graphene flake and solvent molecules depends on the size of flake. As shown in Figure 2D, the probability of finding a water molecule next to the flake edge (around 3.2 Å from the edge) decreases with increasing size of flake. Also, the difference between the interaction strength of oil molecules with flake edge carbon and the surface carbon atoms decreases for bigger flakes. This confirms our predictions that amphipathic strength is greater for smaller flakes.

The additional DFT calculations of multilayered systems (Figure S8, Supporting Information) show that dispersive interactions between stacked flakes considerably reduce the amphipathic strength of single flakes. This also explains why graphite flakes cannot be used to stabilize water/oil emulsions.

The properties of GO stabilized emulsions are also affected by the oil-to-water ratio.<sup>[5]</sup> To investigate whether this is also

true in case of pristine graphene flakes, we performed another solution experiment. The amount of graphene (0.02 g) and water (4 mL) were kept constant while varying the volume of added *n*-decane from 0 to 4 mL (Figure 3A). Figure 3B,C shows the transition between mechanically unstable region where only loose emulsions are formed and the tight emulsions region. The critical point was reached after adding a smaller volume of *n*-decane to water/G3 (0.75 mL) than to water/G1 (1.5 mL) mixtures. To understand this, we have carried out MD simulations of systems containing  $\Gamma_1$  only in water, only in oil, and in two mixtures with different amounts of oil. The RDFs between flake carbon, oil carbon, and water oxygen atoms are shown in Figure 3D. Comparing the systems with and without the oil phase, one can see that the minimal distance between flake carbon and unbound water oxygen atoms is smaller when oil is present in the system but it increases with increasing oil concentration. This minimal distance is equal to 2.57 Å for the system with 15 oil molecules, 3.06 Å for 30 oil molecules and 3.12 Å when no oil is present in the system. On the other hand, the minimal distance between carbon atoms in the flake and carbon atoms in the oil molecules increases with increasing oil concentration (cf. positions of  $C_g$ – $C_{oil}$  RDF first peaks for all systems).

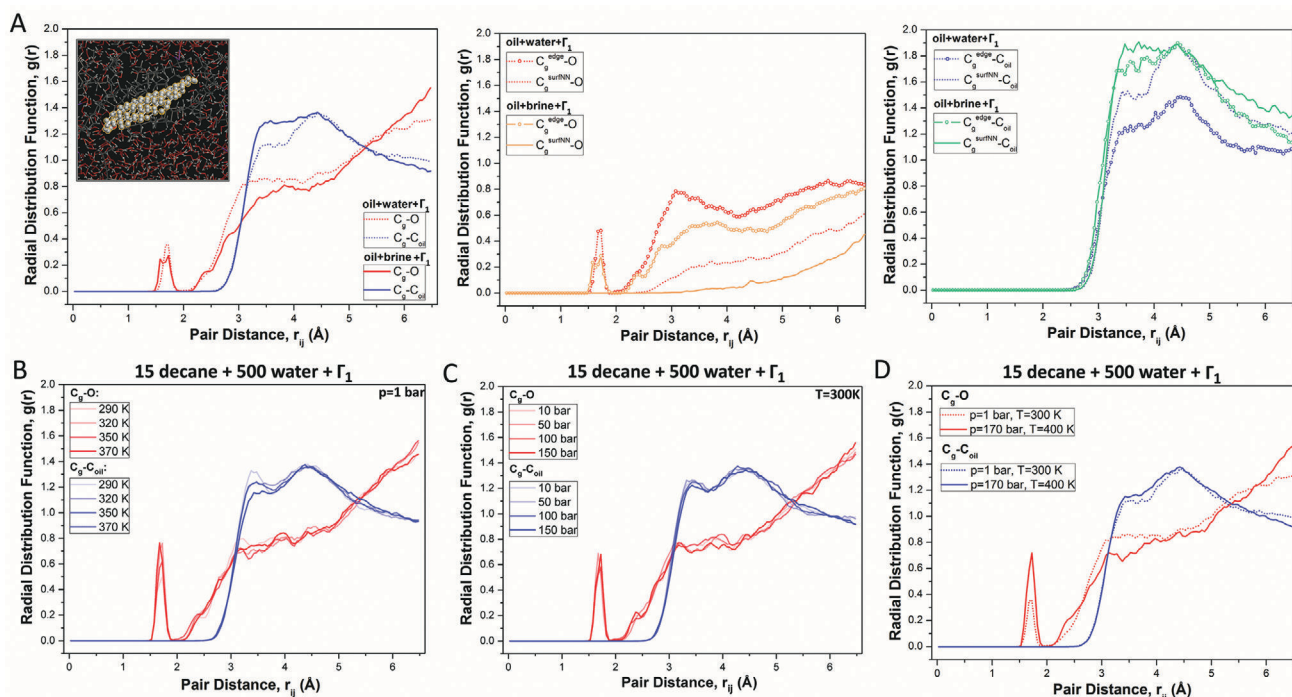


**Figure 4.** Graphene flakes under extreme conditions. A) Interaction of  $\Gamma_1$  flakes in a decane/brine mixture. Left panel: RDF between carbons in a  $\Gamma_1$  flake, oil carbon and water oxygen atoms. The results of a simulation for pure water are also shown. Inset: snapshot of the final configuration of the  $\Gamma_1$  in brine.  $H_2O$ ,  $Na^+$ ,  $Cl^-$ , and *n*-decane are represented using a stick model whereas the graphene flake is displayed as a ball-and-stick model. The C atoms are depicted in gray while O, H, Na, Cl are shown in red, white, violet, and green, respectively. Middle panel: RDF of edge carbon–water oxygen and surface carbon–water oxygen atoms. Right panel: RDF of edge carbon–oil carbon and surface carbon–oil carbon atoms. B–D) Interactions of  $\Gamma_1$  flakes under high under high pressure and high temperature. The data are from MD simulations using pure water. B) RDF for  $\Gamma_1$  flakes at different temperatures. C) RDF for  $\Gamma_1$  flakes at different pressures. D) RDF for  $\Gamma_1$  flakes at  $p = 170$  bar and  $T = 400$  K.

The results of these calculations underpin the argument that interactions between a graphene flake and solvents can be tuned by varying the oil–water ratio.

Next, we have investigated the impact of salt in the water on the behavior of graphene flakes (Figure 4A). Comparison of the MD simulations of systems with and without the additional  $Na^+$  and  $Cl^-$  ions reveals that the presence of salt slightly changes the interaction strength between the graphene flake and both solvents. The presence of salt reduces the distance between oil molecules and the flake, in particular between the oil carbon atoms and the flake edges (cf. positions of first peaks of  $C_g^{edge}-C_{oil}$  RDF in the right panel). Moreover, the number of oil molecules next to the flake surface increases (cf. intensities of first peaks of  $C_g^{surfNN}-C_{oil}$  RDF in the right panel), whereas water molecules are positioned even further from the surface of the flake (cf.  $C_g^{surfNN}-O$  RDF in the middle panel). As a result, oil more tightly coats the surface of the flake. This suggests that salt increases the magnitude of the hydrophobic effect,<sup>[24]</sup> but still, the amphipathic nature of graphene flake is visible. Due to their thermodynamic stability in saline solution and their amphipathic nature, graphene flakes of suitable sizes could conceivably be used, for example, in skin cancer therapy or for antimicrobial and antifungal wound dressings.

For potential industrial applications it is also important to test the stability of any stabilizer under conditions of high temperature and high pressure. The RDFs for  $\Gamma_1$  in water/oil mixtures at different temperatures (Figure 4B) and pressures (Figure 4C)

obtained from MD simulations look similar. As the temperature increases, the first maximum in the  $C_g-C_{oil}$  RDF plots slightly decreases in size and moves toward larger distances. The same trend can be observed for the second maximum in the  $C_g-O$  RDFs which is associated with unbounded oxygen atoms next to the flake. This would suggest that both solvents are pushed further from graphene flakes at higher temperatures.

As one may expect, with increasing pressure, the position of the second peak in the  $C_g-O$  RDFs is shifted toward smaller distances and its magnitude increases. Increasing the pressure from 10 to 50 bars also shifts the first peak of the  $C_g-C_{oil}$  RDFs toward smaller distances and the magnitudes increase. Thus, over this pressure range, compressing the system brings solvent molecules closer to the graphene flakes. This, however, changes when the pressure is further increased. Above 50 bars, the first maximum in the  $C_g-C_{oil}$  RDFs becomes smaller and is shifted toward higher distances. The observed changes are very small. It is apparent that the interactions between the graphene flake and solvent molecules remain relatively unaffected by increase of temperature or pressure. This ability to perform under conditions relevant for geological applications (Figure 4D), where classical stabilizers do not work any longer, means that graphene flakes should continue to function.

Our simple experiments have shown that graphene flakes with the small surface areas can form extremely stable Pickering emulsions. The dispersion of G3 graphene flakes in oil/water mixtures remained unchanged and stable over a long

period of time (Figure S9, Supporting Information), also using other solvents than *n*-decane (Figure S10, Supporting Information). However, the common mixing methods, such as sonication must be used with caution (Figure S11, Supporting Information) since it can crush graphene flake structures.<sup>[5,11]</sup>

To understand the long-term stability of nanostructures, we performed MD and subsequent MC simulations of a few graphene flakes in oil/water mixture. The results (Figure S12, Supporting Information) show that flakes of different sizes can form stacks and/or rotate with respect to each other by an angle close to 90° to expose their edges to the water phase while oil covers their surfaces when they aggregate. This suggests that a small amount of oil under the surfaces of the assembled graphene flakes is needed to stabilize the shell around water droplets in the oil phase.

By combining experimental and theoretical approaches we have demonstrated that graphene flakes are truly 2D amphiphiles with well-defined hydrophilic and hydrophobic regions. For the first time, the DFT calculations have revealed that pristine graphene flakes have hydrophilic edges and hydrophobic basal plane surfaces. In consequence, as molecular dynamic simulations together with experiments indicate, the amphiphatic strength depends on the edge-to-surface ratio of the flake. The relative importance of the hydrophilic edges of the graphene flakes thus decreases with increasing size of the flake. Therefore, only graphene flakes with surface areas in the range which enables a sufficient extent of individualization of the flakes can efficiently stabilize water/oil mixtures. We have also shown that the stability of the water/oil emulsion stabilized by graphene flakes can be tuned by varying the oil-to-water ratio. In addition to the extreme stability of prepared emulsions, we predict that graphene flakes can be efficiently used under high pressure, high temperature and in saline solutions, opening up applications for a broad range of environmental, geological, or biomedical technologies and overcoming many of the limitations of current stabilizers.

## Experimental Section

A detailed description of materials, preparation of emulsions, characterizations, computational studies, and additional analysis can be found in the Supporting Information.

## Supporting Information

Supporting Information is available from the Wiley Online Library or from the author.

## Acknowledgements

A.W.K. and K.Z.M. contributed equally to this work. A.W.K. and K.K.K. acknowledge Cranfield University Grant EME/3022Z. K.Z.M. and M.C.P. acknowledge EPSRC Grant EP/P034616/1. S.B. is very grateful for the financial support from the National Science Centre (Poland) Grant No. 2019/33/B/ST5/01412 in the framework of OPUS program. S.B. also greatly acknowledges financial support in the area of fundamental sciences and R&D from Silesian University of Technology Rector's Grant No. 892/RN2/RR42019. P.-L.C. was partly supported by the INCEPTION project ANR-16-CONV-0005.

## Conflict of Interest

The authors declare no conflict of interest.

## Keywords

graphene flakes, interfacial self-assembly, Pickering emulsions, stabilizers

Received: January 27, 2020

Revised: June 1, 2020

Published online: July 16, 2020

- [1] K. S. Novoselov, A. K. Geim, S. V. Morozov, D. Jiang, Y. Zhang, S. V. Dubons, I. V. Grigorieva, A. A. Firsov, *Science* **2004**, 306, 666.
- [2] a) A. K. Geim, *Science* **2009**, 324, 1530; b) T. Reiss, K. Hjelt, A. C. Ferrari, *Nat. Nanotechnol.* **2019**, 14, 907.
- [3] J. Texter, *Curr. Opin. Coll. Int. Sci.* **2015**, 20, 454.
- [4] T. M. McCoy, G. Turpin, B. M. Teo, R. F. Tabor, *Curr. Op. Coll. Int. Sc.* **2019**, 39, 98.
- [5] Y. He, F. Wu, X. Sun, R. Li, Y. Guo, C. Li, L. Zhang, F. Xing, W. Wang, J. Gao, *ACS Appl. Mater. Interfaces* **2013**, 5, 4843.
- [6] L. Horvath, B. Schwaller, A. Magrez, M. Burghard, K. Kern, L. Forro, *Carbon* **2013**, 64, 45.
- [7] J. P. Rourke, P. A. Pandey, J. J. Moore, M. Bates, I. A. Kinloch, R. J. Young, N. R. Wilson, *Angew. Chem. Int. Ed.* **2011**, 50, 3173.
- [8] a) W. Zhao, F. Wu, H. Wu, G. Chen, *J. Nanomater.* **2010**, 528235; b) S. Haar, M. E. Gemayel, Y. Shin, G. Melinte, M. A. Squillaci, O. Ersen, C. Casiraghi, A. Ciesielski, P. Samori, *Sci. Rep.* **2015**, 5, 16684; c) L. Xu, J. McGraw, F. Gao, M. Grundy, Z. Ye, Z. Gu, J. Shepherd, *J. Phys. Chem. C* **2013**, 117, 10730.
- [9] L. Belyaeva, P. van Deursen, K. Barbetsea, G. Schnerider, *Adv. Mater.* **2018**, 30, 1703274.
- [10] B. Robinson, N. Kay, O. V. Kolosov, *Langmuir* **2013**, 29, 7735.
- [11] V. Shabafrooz, S. Bandla, J. Hanan, *J. Mater. Sci.* **2018**, 53, 559.
- [12] S. J. Woltornist, J.-M. Y. Carrillo, T. O. Xu, A. V. Dobrynin, D. H. Adamson, *Macromolecules* **2015**, 48, 687.
- [13] M. J. Large, S. P. Ogilvie, M. Meloni, A. A. Graf, G. Fratta, J. Salvage, A. A. K. King, A. B. Dalton, *Nanoscale* **2018**, 10, 1582.
- [14] S. J. Woltornist, A. J. Oyer, J.-M. Y. Carrillo, A. V. Dobrynin, D. H. Adamson, *ACS Nano* **2013**, 7, 7062.
- [15] a) B. P. Binks, S. O. Lumsdon, *Langmuir* **2000**, 16, 8622; b) Y. Yang, Z. Fang, X. Chen, W. Zhang, Y. Xie, Y. Chen, Z. Liu, W. Yuan, *Front. Pharmacol.* **2017**, 8, 287.
- [16] L. J. Cote, J. Kim, V. C. Tung, J. Luo, F. Kim, J. Huang, *Pure Appl. Chem.* **2011**, 83, 95.
- [17] Y. S. Kim, S. J. Yang, H. J. Lim, T. K. Chong, R. Park, *Carbon* **2012**, 50, 3315.
- [18] N. Bonatout, F. Muller, P. Fontaine, I. Gascon, O. Konovalov, M. Goldmann, *Nanoscale* **2017**, 9, 12543.
- [19] D. Lungerich, O. Papaianina, M. Feofanov, J. Liu, M. Devarajulu, S. I. Troyanov, S. Maier, K. Amsharov, *Nat. Comm.* **2018**, 9, 4765.
- [20] W. Yuan, Y. Zhou, Y. Li, C. Li, H. Peng, J. Zhang, Z. Liu, L. Dai, G. Shi, *Sci. Rep.* **2013**, 3, 2248.
- [21] J. Kim, L. J. Cote, J. Huang, *Acc. Chem. Res.* **2012**, 45, 1356.
- [22] J. Kim, L. J. Cote, F. Kim, W. Yuan, K. R. Shull, J. Huang, *J. Am. Chem. Soc.* **2010**, 132, 8180.
- [23] A. R. Koltonow, J. Kim, L. J. Cote, J. Luo, J. Huang, *Mater. Res. Soc. Symp. Proc.* **2011**, 1344, 93.
- [24] a) R. L. Mancera, *J. Chem. Soc., Faraday Trans.* **1998**, 94, 3549; b) R. L. Mancera, *Chem. Phys. Lett.* **1998**, 296, 459.